Imaging of the cardiorenal syndrome and visceral fat

Lin, L.

Chapter 2

Fat Accumulation around and within the Kidney

Lin L, Dekkers IA, Lamb HJ.
Visceral and Ectopic Fat, edited by Lamb HJ. Elsevier. *In press*.

ABSTRACT

Excessive adipose tissue can accumulate not only around the kidneys in the form of perirenal fat and renal sinus fat, but also within the kidney as lipid droplets in parenchymal cells. Kidney adipose tissue functions as a paracrine and endocrine organ and can contribute to the dysregulation of kidney function, lipids metabolism, gluconeogenesis and cardiovascular function if presents in excess. Non-invasive quantification of the fat around and within the kidney has been enabled by imaging modalities including ultrasonography, computed tomography and magnetic resonance imaging, and has been investigated in various clinical studies. These studies suggest that perirenal fat, renal sinus fat and intrarenal fat may have a potential role in the development of obesity-related chronic kidney disease, insulin resistance, hypertension and atherosclerosis. Large-scale longitudinal studies are warranted to evaluate the utility of these imaging biomarkers in clinical practice in the future.

INTRODUCTION

The kidneys are surrounded by perirenal fat, which separates the kidney capsule and kidney facia. Around the renal hilum, perirenal fat extends along renal arteries, veins, lymphatic vessels, nerve fibers and collecting system, and fills the renal sinus with renal sinus fat. In addition, lipids can accumulate in the kidney parenchyma in obese status (also referred to as "fatty kidney"), mainly in the tubules and glomeruli. Fat accumulation around and within the kidney participates in the regulation of kidney function, energy metabolism, gluconeogenesis and cardiovascular function through paracrine and endocrine pathways. Excessive kidney fat is associated with a number of clinical implications, such as chronic kidney disease, diabetes mellitus, hypertension, atherosclerosis, kidney neoplasm, etc. In this chapter, the anatomical, histological and physiological characteristics of perirenal fat, renal sinus fat and fat deposition in the renal parenchyma are described. Non-invasive quantification of these fat compartments using imaging modalities as well as their clinical implications are elaborated in this chapter.

PERIRENAL FAT AND RENAL SINUS FAT

Anatomical characteristics

Perirenal fat is located around the kidneys and the adrenal glands, and is separated from the pararenal fat in the retroperitoneal space by a condensed, membranous layer of renal fascia. Rena fascial encloses (except inferiorly) perirenal fat with the anterior fascia of Gerota (1) and the posterior fascia of Zuckerkandl (2) (**Figure 2.1**). The anterior renal fascia is thin and on occasions elusive, while the posterior renal fascia is tough. Laterally the anterior fascia and the posterior fascia merge and form the lateroconal fascia. Medially the anterior fascia and the posterior fascia extend to midline, fuse with the vascular sheaths of the renal vessels, and at midline the left and right renal fascia fuse anterior to the aorta and the inferior vena cava (**Figure 2.2**). However, this fusion has a defect below the level of renal hilum, which enables a potential communication across the midline between the two perirenal spaces (3). There is a thin fascial plane between the adrenal gland and the kidney, but cranially the anterior fascia and the posterior fascia fuse above the adrenal gland and mix imperceptibly with the diaphragmatic facia (4). Unlike the lateral, medial and superior part of the perirenal space, the inferior compartment is not completely closed. Part of the renal facia merges with the ureteral sheath and part ends subtly within the retroperitoneal fat. A cadaver study using

computed tomography (CT) found that contrast medium injected into the perirenal space tracked down to the pelvic extraperitoneal and presacral spaces, suggesting a communication between the caudal extremity of the perirenal space and the posterior pararenal space (3). Inside the perirenal space, there are sparse strands of connective tissue in addition to adipose tissue (5). In summary, the upper part of perirenal fat that is separated from pararenal fat and other retroperitoneal structures by a complete renal fascia, while the lower part of perirenal fat has the shape of an inverted cone but not completely enclosed by the renal facia, with potential communication with the pelvis and the opposite side across the midline (**Figure 2.3**).

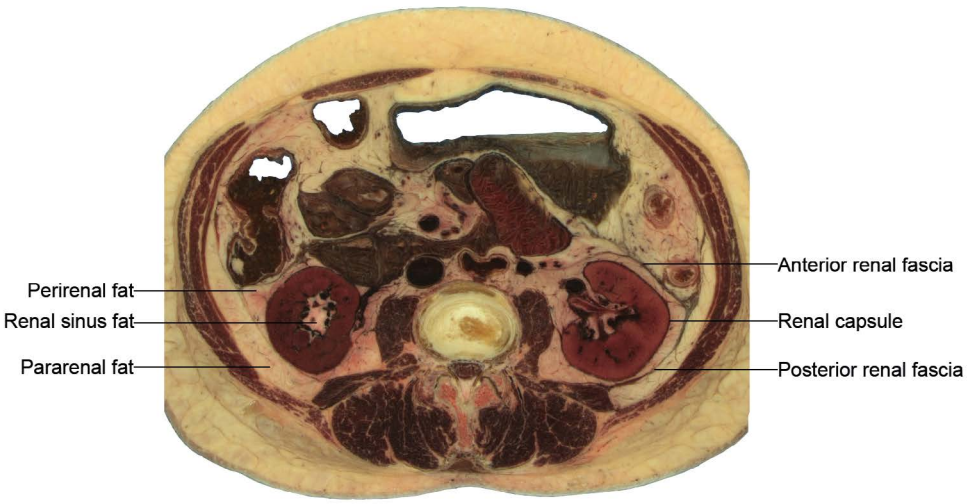

Figure 2.1 Cross-sectional view of the fat around the kidneys. Adapted from a photo of a female cadaver from the Visible Human Project at https://www.nlm.nih.gov/research/visible/visible_human.html.

Perirenal fat is well-vascularized by an anastomosing capillary network generated from the branches of the inferior suprarenal, left colic, renal, lumbar, and ovarian/testicular arteries (6, 7). Perirenal lymphatic vessels communicate extensively with renal subcapsular lymphatic vessels and eventually drain into the para-aortic lymph nodes (8). Perirenal fat is also richly innervated. Animal studies have revealed that perirenal nerve fibers originate from the celiac-superior mesenteric ganglion, ipsilateral inferior mesenteric ganglion, adrenal ganglion, aorticorenal ganglion, gonadal ganglion, and L1–L3 ipsilateral sympathetic trunk ganglia (9, 10).

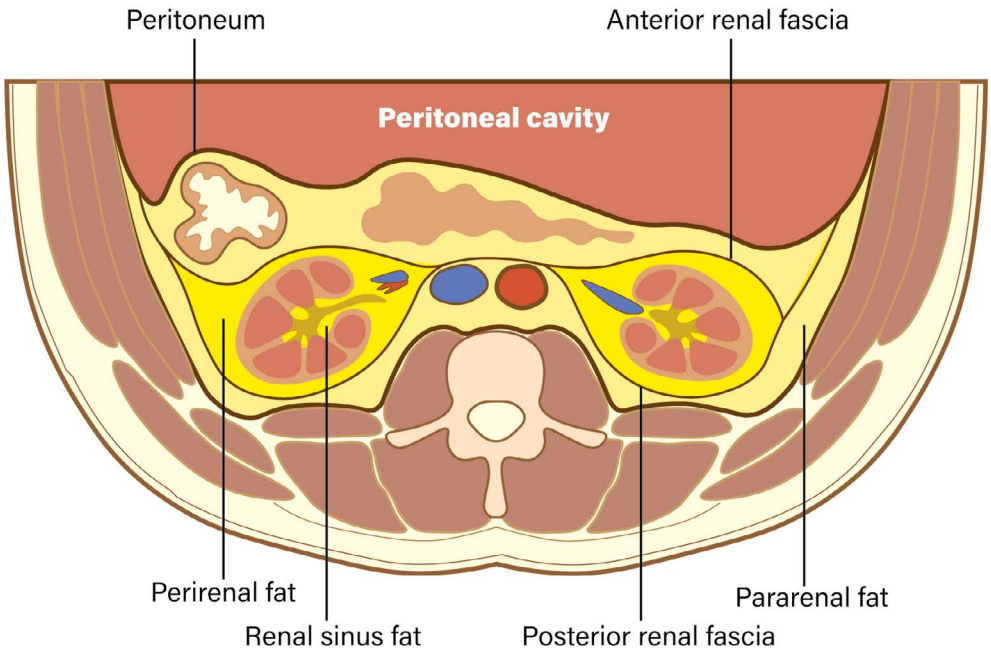

Figure 2.2 Schematic diagram of renal fascia, perirenal fat and renal sinus fat in a transversal view.

Renal sinus fat is the extension of perirenal fat starting around the renal hilum and intrudes upon the renal parenchyma (**Figure 2.1-2.3**). Renal sinus fat is separated from the renal parenchyma by the reflection of the renal capsule (11). As there is no anatomical separation between renal sinus fat and perirenal fat, renal sinus fat is considered as a component of perirenal fat. Renal sinus fat is in close contact with the renal pelvis, calyces, renal vasculatures, lymphatic vessels and nerve fibers. Therefore, renal sinus fat is also considered as a perivascular adipose tissue, which may contribute to the pathogenesis of cardiovascular diseases like other perivascular adipose tissue, such as epicardial fat (12). However, it has not been confirmed whether renal sinus fat is physiologically and functionally different from the general perirenal fat, due to the lack of histological studies specific to sinus fat.

Both perirenal fat and renal sinus fat can be found in lean individuals (13-15). The amount of perirenal fat and sinus fat varies with different individuals and metabolic conditions (**Figure 2.4**). In a population aged 21-80 years old without renal diseases, renal sinus fat volume was found to increase with age, though it appeared to decrease in individuals older than 70 years of age (13). Sex difference in the distribution of perirenal fat has been reported in previous studies, in which the thickness of perirenal fat measured on cross-sectional computed tomography (CT) images was larger in men

than that in women (16, 17). Another study found larger perirenal fat volume in men compared with women of comparable waist circumference (18). Similarly, smaller renal sinus fat area was found in women than in men (18). This study also found that the area of renal sinus fat derived from a single-slice CT image was correlated with the volume of perirenal fat, however not as strongly as the perirenal fat thickness correlated with perirenal fat volume (18). Two studies found that renal sinus fat compartments distribute asymmetrically, with more fat accumulation in the left renal sinus than in the right (13, 19). Therefore, it is recommended to assess the left-side renal sinus fat for a more reliable observation (19).

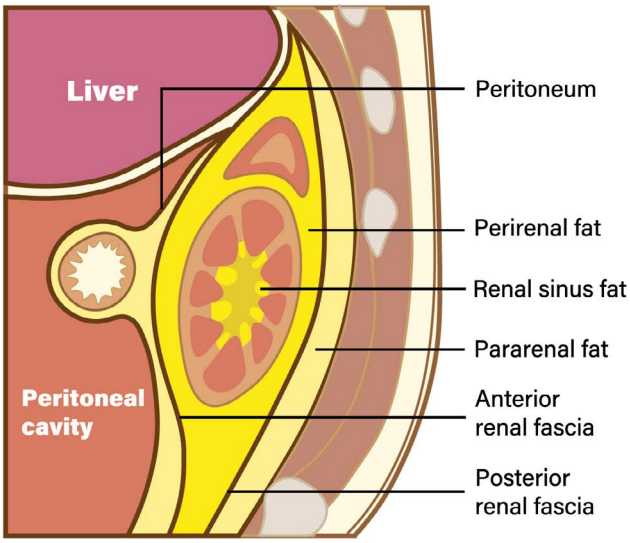

Figure 2.3 Schematic diagram of renal fascia, perirenal fat and renal sinus fat in a sagittal view. The lower part of perirenal fat is not completely enclosed by the renal facia, with potential communication with the pelvis.

Currently no standards or consensus is available for the definitions of excessive perirenal fat and renal sinus fat. In the general population, sinus fat volume in one kidney has been described to range from 0.07 cm^3 to 11.23 cm^3 (19). Perirenal fat thickness was found to be correlated with body mass index (BMI) (16). However, it was also observed that obese individuals did not necessarily have proportionally increased perirenal fat when compared to individuals with lower BMI (16). In obese rabbits and humans, renal sinus fat is associated with kidney size (14, 20, 21). In contrast to our recent findings that renal sinus fat volume derived from magnetic resonance imaging (MRI) was correlated with body size (14), no correlation was found between renal sinus fat area and any anthropometric measurements in a previous study (18). Moreover,

renal sinus fat volume was found to be positively associated with abdominal visceral adipose tissue (VAT) in individuals with prediabetes or diabetes (14, 22) (**Figure 2.5**).

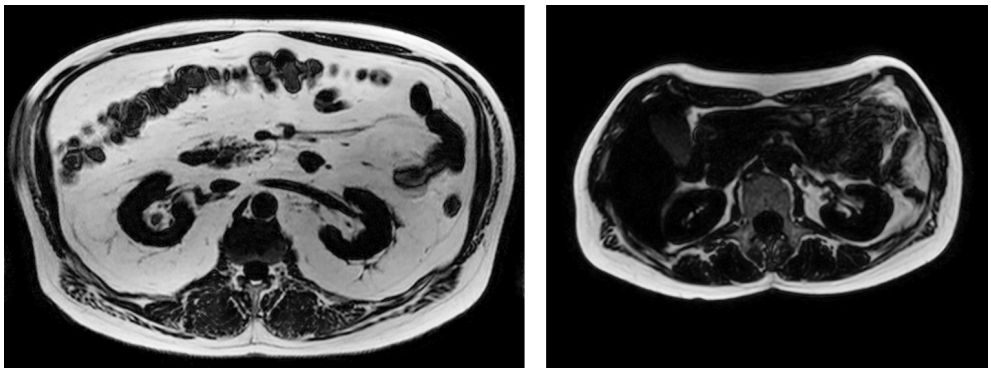

Figure 2.4 Dixon fat-only images showing much larger amount of perirenal fat and renal sinus fat in an obese patient with diabetes (left) than that in a lean healthy volunteer (right).

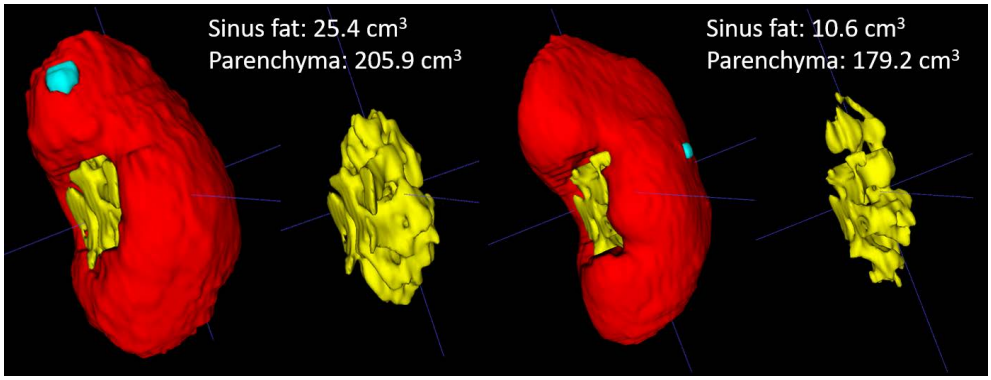

Figure 2.5 A patient with type 2 diabetes mellitus (left) had larger renal sinus fat volume than a healthy control (right) of similar body size. Renal parenchyma volume and sinus fat volume were obtained from Dixon images, where sinus fat was labeled yellow, and cysts (blue) were excluded from the calculation of parenchyma volume (red). Left: a 64-year male patient with type 2 diabetes mellitus whose height was 178.0 cm and weight was 86.9 kg. Right: a 61-year healthy male whose height was 178.5 cm and weight was 85.7 kg.

Histological and pathophysiological characteristics

Currently the adipose tissue around the kidneys is considered as a special deposit of abdominal VAT, which shares the same developmental origin of VAT. However, the

histological, physiological and functional characteristics of ectopic renal adipose tissue are different from those of VAT in other anatomical locations (23). Interestingly, a recent study of human adipose tissue found that the gene expression profile of perirenal adipose tissue was more analogous to that of subcutaneous adipose tissue (SAT) than VAT, but perirenal fat can still be distinguished from SAT according to different expression patterns (24).

Different from typical abdominal VAT which mainly consists of white adipocytes, perirenal adipose tissue is a mixture of white, brown and beige adipocytes. In fetuses and infants (1-11 months of life), perirenal fat is predominantly composed of brown adipocytes (25). After birth, the amount of brown adipose tissue is decreased due to a progressive transition into white adipose tissue. Only a small portion of brown adipocytes with multilocular morphology remain active in perirenal fat in adults, mainly located in areas richly innervated by sympathetic nerve fibers, for instance, around the renal hilum and near the adrenal gland (26). However, It has been observed that most of the perirenal fat in adults consists of unilocular dormant brown adipocytes, which are different from multilocular brown adipocytes and are evenly distributed in perirenal adipose tissue (26). Gene analysis suggested that the majority of human perirenal adipocytes express the genes of uncoupling protein-1 (UCP1), a protein unique to brown adipocyte mitochondria (27). However, there is a significant individual variability in the portion of UCP1-positive adipocytes in perirenal fat (27). One study of a Siberia population who live in the coldest regions of the earth found higher percentage of brown adipocytes with more intensely expression of functional UCP1 in individuals living mainly outdoor, supporting the idea that perirenal adipose tissue can be converted to brown adipose tissue in cold conditions (28). Sex difference in perirenal fat has also been reported by histological studies (29, 30). Mesenchymal stem cells derived from female perirenal adipose tissue express significantly more UCP1 mRNA than those from male perirenal adipose tissue, indicating that women have more potential to induce "browning" of perirenal fat than men (29). The underlying mechanism could be the association between the number of X chromosomes and adiposity rather than the effects of sex hormones, as suggested by a murine study (30).

The unique component adipocytes form the basis for the physiological and functional characteristics that distinguish perirenal fat from other VAT deposits (31, 32). Perirenal fat functions as an active paracrine and endocrine organ, synthesizing and secreting a number of adipokines and inflammatory cytokines pertinent to energy metabolism and inflammation (33). Perirenal fat participates in the regulation of kidney function, glucose and lipid metabolism and cardiovascular homeostatic function by several physiological pathways including sympathetic activation, humoral regulation, renin-

angiotensin system and inflammation (33). The underlying mechanisms of how perirenal fat contributes to chronic kidney disease, hyperglycemia, hypertension and atherosclerosis have been summarized in recent publications (6, 8, 33, 34).

Imaging-based quantification

Similar to other VAT compartments, accumulation of perirenal fat and renal sinus fat can be evaluated by imaging modalities including ultrasonography, CT and MRI. Perirenal fat is mostly measured by ultrasonography and CT, while renal sinus fat is mainly quantified by CT and MRI. **Table 2.1** provides a list of studies and the corresponding imaging modalities used for quantifying perirenal fat and sinus fat in humans.

Quantification of perirenal fat

While ultrasonography is most widely used in clinical studies to measure the thickness of perirenal fat, it is operator-dependent and the measurements are limited by the location of the acoustic window. The most frequently used acoustic window is the longitudinal scanning on the lateral aspect of the abdomen in the supine position, at which the surface of the kidney was almost parallel to the skin (15, 35-43). However, the problem of this method is that not only the thickness of perirenal fat is measured, but also the pararenal fat between the renal fascia and the inner side of abdominal musculature, which is retroperitoneal adipose tissue, is included (**Figure 2.6**). Moreover, the pressure exerted by the probe might also impact the measurements. An alternative acoustic window adopted by a few studies was the longitudinal scanning along the midclavicular line, and the anterior distance from the border of the liver/spleen to the border of the inferior part the kidney was measured as the thickness of perirenal fat (44-46) (**Figure 2.7**).This method can exclude the impact of pararenal fat, but has not been widely used. Intra-observer reproducibility of the ultrasonographic measurement of perirenal fat thickness was evaluated in several earlier studies, with coefficient of variance ranging from 3.2% to 6.5% (35-39, 44, 45). Interobserver reproducibility was evaluated in only one study, presenting an interobserver intraclass correlation of 0.51 (40). There was also one study placing the probe at the axillary midline in the longitudinal plain, where the posterior measurement of the lateral hypoechoic area was taken as the thickness of perirenal fat (47). The reproducibility of this method was not evaluated, and this method has not been adopted by other studies.

Table 2.1 Overview of human studies using imaging modalities for the quantification of perirenal fat and renal sinus fat.

	Perirenal fat		Renal sinus fat	
Imaging modality	List of studies	Measurement	List of studies	Measurement
Ultrasound	Lamacchia, et al. 2010 (35); Sun, et al. 2013 (36); Sahin, et al. 2015 (37); De Pergola, et al. 2015 (38); Bassols, et al. 2018 (15); Geraci, et al. 2018 (39); Ricci, et al. 2018 (40); López-Bermejo, et al. 2019 (41); Manno, et al. 2019 (42); Fang, et al. 2020 (43)	Thickness of perirenal + pararenal fat	None	Not applicable
	Grima, et al. 2010 (44, 45); D'Marco, et al. 2019 (46); Roever al al. 2015 (47);	Thickness		
CT	Favre et al. 2017 (48); Eisner, et al. 2010 (16); Anderson, et al. 2008 (17); Koo, et al. 2020 (49); Chen et al. 2021 (50); Ji, et al. 2017 (51)	Thickness	Favre et al. 2017 (48); Foster, et al. 2011 (52)	Single-slice area
	Favre et al. 2017 (48); Lama, et al. 2018 (53); Maimaituxun, et al. 2019 (54)	Volume	Foster, et al. 2011 (52); Caglar, et al. 2014 (13); Krievina, et al. 2016 (19); Murakami, et al. 2016 (55); Lin, et al. 2020 (56)	Volume
MRI	None	Not applicable	Wagner, et al. 2012 (57); Wagner, et al. 2017 (58); Zelicha, et al. 2018 (59); Spit, et al. 2020 (60);	Single-slice area
			Chughtai, et al. 2010 (20)	Single-slice volume
			Notohamiprodjo, et al. 2020 (22) Lin, et al. 2021 (14)	Volume

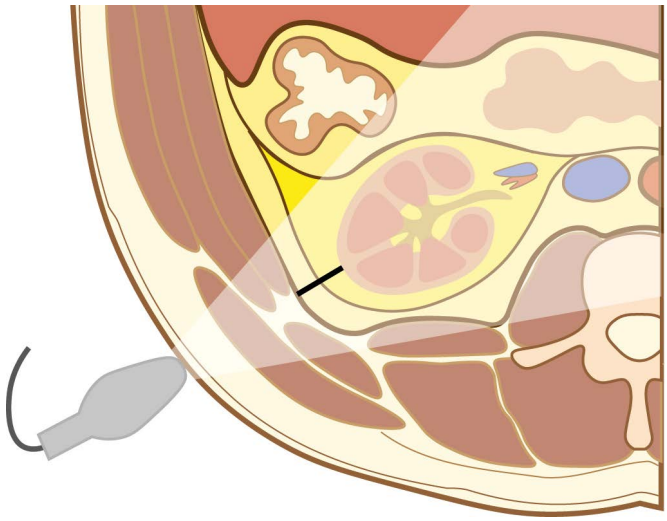

Figure 2.6 Schematic diagram showing the measurement of perirenal fat thickness on the lateral aspect of the abdomen using ultrasound. This method measures the sum of perirenal fat thickness plus pararenal fat thickness in the acoustic window (black line).

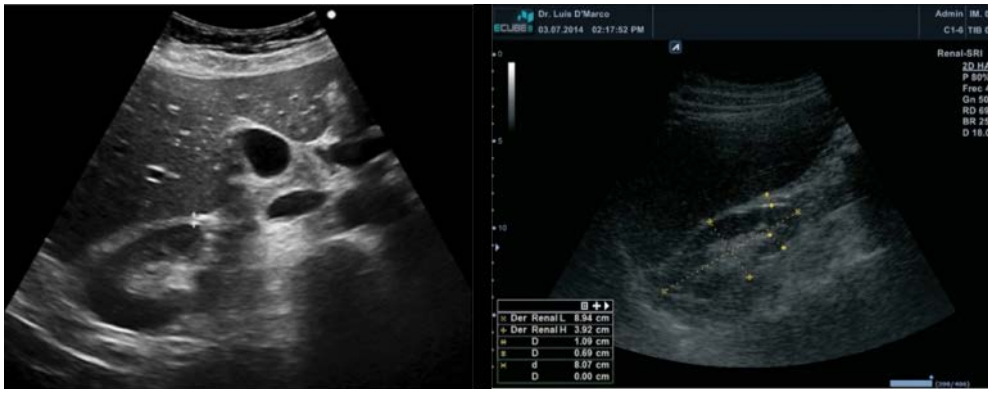

Figure 2.7 Measurement of perirenal fat thickness using ultrasound along the midclavicular line. The thickness of perirenal fat is the anterior distance from the border of the liver to the border of the inferior part of the kidney. Images were adapted from published articles (44, 46) under a Creative Commons license.

CT and MRI images can also be used to evaluate perirenal fat. However, these imaging modalities are more expensive and less accessible than ultrasonography. Earlier studies using CT to quantify perirenal fat were mainly conducted in patients who underwent nephrectomy. The renal fascia is not always visible on CT images, especially the anterior

fascia, which can be elusive or closely adjacent to pararenal structures, such as small intestines, colon, spleen and liver. It is often impossible to accurately delineate the complete renal facia, especially in less obese subjects. Therefore, the thickness of perirenal fat was measured in a number of studies instead of volumetric evaluation. However, the thickness of perirenal fat varies significantly with locations in different individuals (**Figure 2.8**), and there is no expert consensus on where and how to measure the perirenal fat thickness. One previous study measured the anterior, posterior, lateral, anterolateral, posterolateral and medial perirenal fat thicknesses at the level of renal vein, among which the correlations with BMI and the gender differences were not consistent (16). A recent study also measured the perirenal fat thickness at multiple locations on the slice passing through the renal vein, and the total perirenal fat thickness was defined as the sum of all the thicknesses on both sides (49). Although one study suggested that perirenal thickness was a reliable estimate of perirenal mass, based on the Pearson's correlation coefficient (r = 0.86) between the posterior thickness and the volume of perirenal fat excluding renal sinus fat (48), the perirenal fat thickness in this study was the maximal distance between the posterior surface of the kidney and the inner margin of the abdominal wall, which also included the thickness of pararenal retroperitoneal fat.

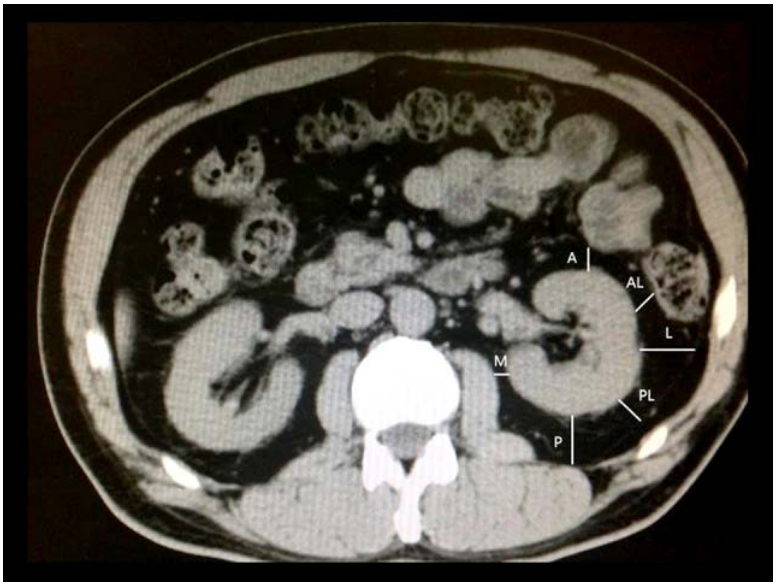

Figure 2.8 The thickness of perirenal fat varies significantly with the locations of measurements. A, anterior; M, medial; L, lateral; AL, anterolateral; PL, posterolateral; P, posterior. Reprinted from a published article (51) with permission from Elsevier.

Quantification of renal sinus fat

The ectopic accumulation of renal sinus fat was referred to as renal sinus lipomatosis in early studies (61, 62). Although ultrasonographical assessment of renal sinus fat is technically feasible, it has not been used for clinical studies regarding excessive sinus fat. Both CT and MRI have been adopted by previous studies for the quantification of the single-slice area or the volume of renal sinus fat based on Hounsfield Units in CT or signal intensity in MRI (**Figure 2.9**). As aforementioned in this chapter, there is no anatomical separation between renal sinus fat and perirenal fat, thus the quantification of sinus fat requires an artificial border. A widely accepted border of renal sinus fat is defined by a straight line tangent to the parenchyma on both sides of the hilum at a transversal slice (13, 14) (**Figure 2.10**). Other definitions such as "a straight line tracing across both dimples at the edge of the renal sinus (52, 56), "a space within the concavity of kidney" (20), and "within the curvature of the kidney" (60), have also been used. Due to the highly irregular shape and the small volume of renal sinus fat, it is preferable to exclude visible vasculatures and the collecting system within the renal sinus. The volume of renal sinus fat can be obtained by multiplying the area of renal sinus fat and thickness of each slice, and adding up the volumes of a series of consecutive slices covering the range of the renal sinus (**Figure 2.10, 2.11**).

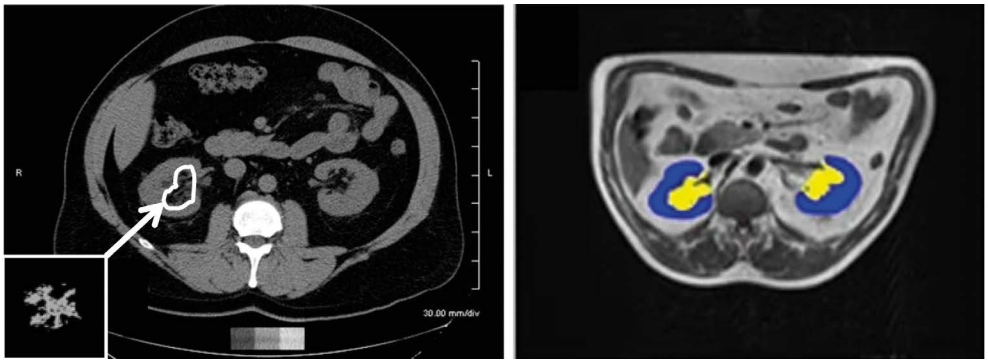

Figure 2.9 Quantification of renal sinus fat based on Hounsfield Units in CT (left) or signal intensity in T1-weighted MRI (right). Images were adapted from published articles (52, 58) under a Creative Commons license.

The feasibility and high reproducibility of measuring single-slice area of renal sinus fat as well as sinus fat volume on CT was firstly presented in a sample from the Framingham cohort (52). In this study the single-slice area and the volume of renal sinus fat were similarly correlated with BMI, waist circumference and abdominal VAT.

Renal sinus fat quantification based on MRI was firstly performed in a study of 205 participants with cardiovascular risk factors, in which the volume of a single-slice renal sinus fat was obtained at the level of the second lumbar vertebra (20). Another study measured the area of renal sinus fat at the level of the entry of the renal arteries (57). MRI quantification of single-slice area of sinus fat is most frequently performed on T1-weighted image, in which the hyperintense sinus fat can be differentiated from the isointense kidney parenchyma (58) (**Figure 2.9**).

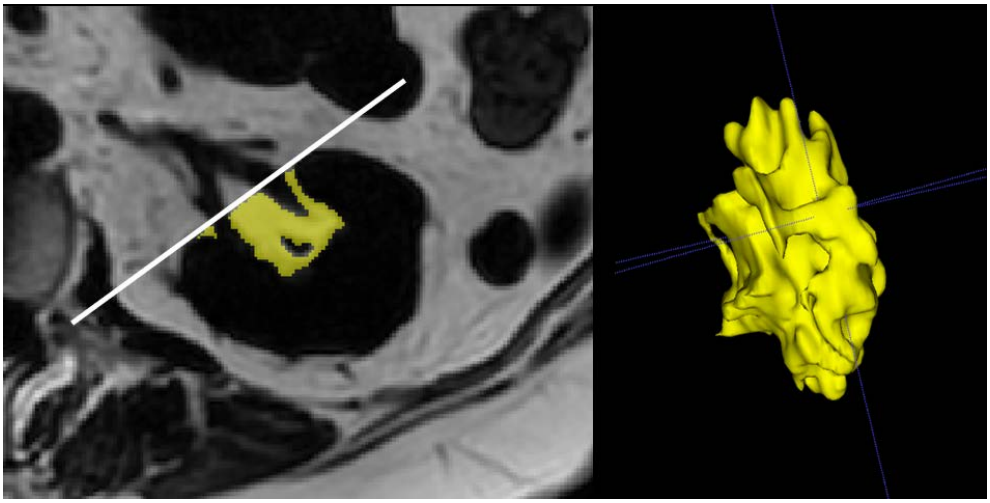

Figure 2.10 Quantification of renal sinus fat based on MRI. The left image shows the segmentation of renal sinus fat on a Dixon-fat image. The border of renal sinus fat is defined by a straight line (white line) tangent to the parenchyma on both sides of the hilum at a transversal slice. The right image is the three-dimensional reconstruction of the sinus fat.

Volumetric evaluation of renal sinus fat on CT have been studied in a population aged 21-80 years old without renal diseases (13), as well as in a group of asymptomatic middle age (30-45 years old) participants (19). With the increased application of high-resolution Dixon imaging in clinical MRI (63), accurate measurement of sinus fat volume based on Dixon images has been feasible (**Figure 2.10**) with high intra- and inter-rater reproducibility (14, 22) (**Figure 2.12**).

Based on previous studies and the features of each imaging modality, there are a few considerations for future studies regarding imaging-based quantification of perirenal fat and renal sinus fat. Perirenal fat is frequently quantified by thickness due to the challenge of delineating the renal fascia, and ultrasonography is the most widely used imaging modality. However, the interobserver reproducibility is largely unknown and

may be impacted by operator-dependence, which is one of the major disadvantages of ultrasonography. Moreover, significant variance of the perirenal fat thickness and the involvement of pararenal fat in the measurement further compromises the accuracy of this quantification method. As for renal sinus fat, volumetric measurement is recommended due to its small size and highly irregular shape, and high intra- and inter-observer reproducibility using CT and MRI has been reported. Considering the radiation risk from CT, renal sinus fat volume quantified by MRI might be preferable over other methods in evaluating the fat accumulation around the kidneys.

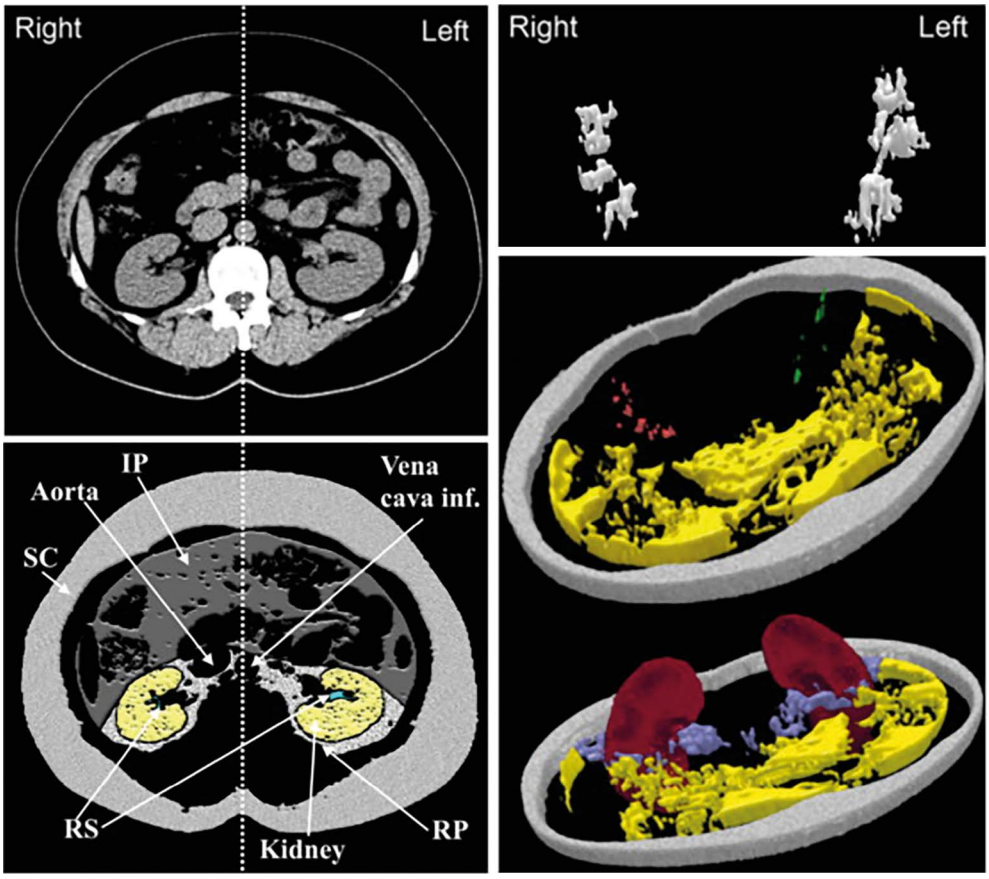

Figure 2.11 Volumetric analysis of renal sinus fat and the other adipose compartments by CT. The left two images show the segmentation of renal sinus fat (RS), intraperitoneal adipose tissue (IP), subcutaneous adipose tissue (SC) and retroperitoneal adipose tissue (RP). The right two images show the three-dimensional reconstruction of the left and right renal sinus fat (right top) and the other adipose compartments (right bottom). Reprinted from a published article (19) under a Creative Commons license.

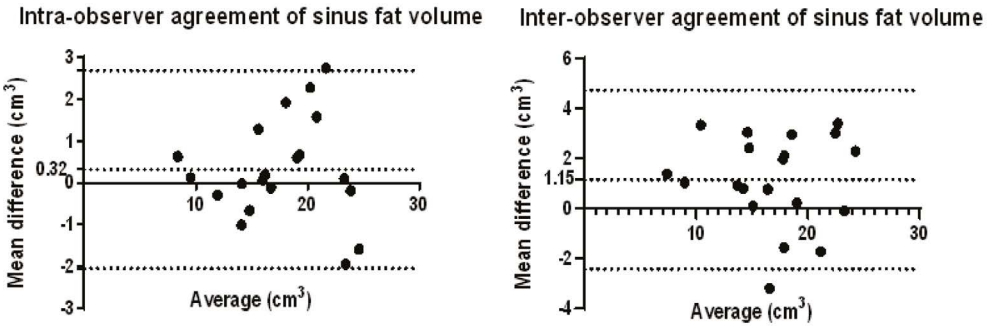

Figure 2.12 Intra- and inter-observer reproducibility of sinus fat volume was high based on high-resolution MRI. Adapted from Lin et al. (14) under the terms of the Creative Commons.

RENAL PARENCHYMA TRIGLYCERIDE

Excessive adipose tissue not only accumulates around the kidney but also increases the amount of lipid droplets inside the renal parenchymal cells. The infiltration of lipids in the kidney, also known as "fatty kidney" or renal steatosis, has been recognized for more than a century (64). Intra-renal fat deposits in the glomeruli and proximal tubules interfere with the metabolism of lipids and glucose, and contribute to kidney injury as well as insulin resistance (34).

Histological characteristics and pathophysiological relevance

Non-esterified fatty acids (NEFA) produced by abdominal adipose tissue plays a key role in the accumulation of lipids in renal cells. More than 99% circulating NEFA is bounded with plasma albumin, and is carried to the liver where synthesis of very low density lipoprotein is stimulated. Intracellular re-esterification results in the production of excessive triglycerides that can be delivered to non-adipose peripheral tissue (65). During this process, modified low density lipoprotein (LDL) (small dense LDL or oxidized LDL) is generated and can lead to intracellular accumulation of cholesteryl esters in cells with scavenger receptors (66). Both triglycerides and cholesteryl esters can be stored in kidney cells by means of lipid droplets, which are coated with a monolayer of phospholipid and regulatory proteins such as adipophilin (67). Extensive lipid droplets can accumulate in mesangial cells, podocytes and proximal epithelial tubular cells, as revealed by histological studies of renal samples from patients with obesity-related glomerulopathy or metabolically unhealthy obesity (67). The impact of lipids accumulation on renal cellular structure and function varies with the types of

renal cells, which has been thoroughly elucidated in a previous review (**Figure 2.13**) (68), and is briefly summarized below.

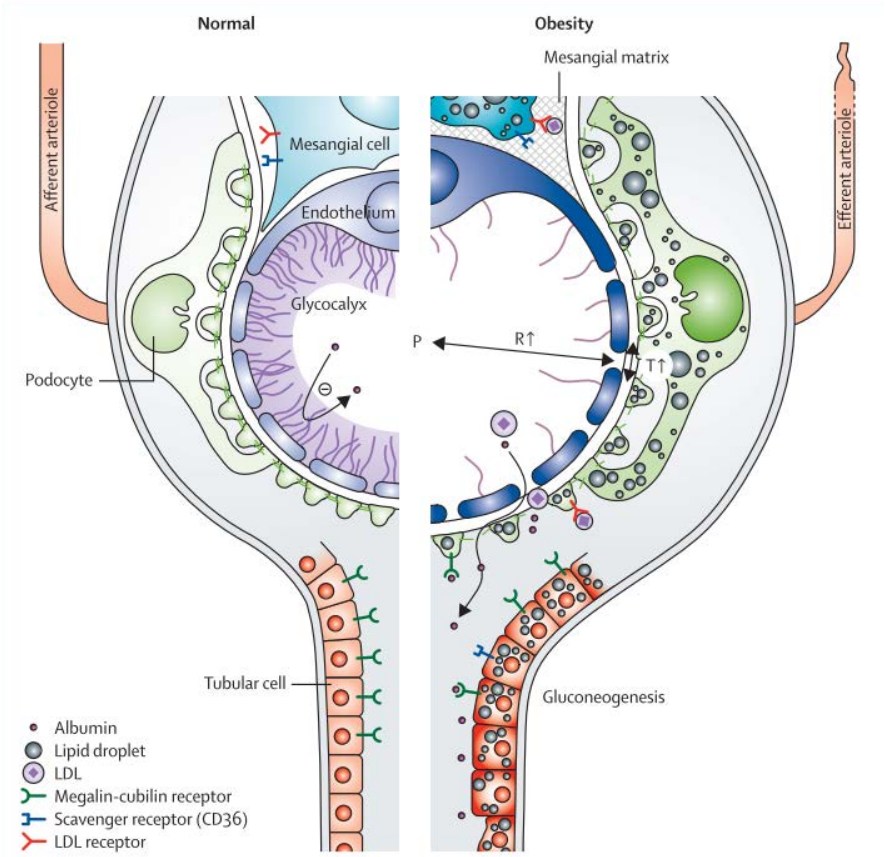

Figure 2.13 Lipid droplets accumulate in mesangial cells, podocytes and proximal tubular epithelial cells and contribute to glomerulomegaly, glomerulosclerosis and enhanced gluconeogenesis. Reprinted from a published article (68) with permission from Elsevier.

Mesangial cells are the specialized microvascular pericyte in the renal glomerulus and are in direct contact with lipoproteins, as there is no basal membrane between mesangium and glomerular endothelium. Obesity-induced endothelial dysfunction can lead to increased lipoprotein leakage, which results in the accumulation of lipids in mesangial cells (69, 70). Moreover, normal feedback regulation in mesangial cells is disrupted by inflammation, which leads to the transformation of mesangial cells to lipid-laden foam cells (71, 72). This transformation of mesangial cells results in the loss of contractile function and contributes to glomerulomegaly (68).

Accumulation of ectopic lipids including NEFA, cholesteryl esters and fatty acids in podocytes has been linked to podocyte-specific insulin resistance (68, 73) and apoptosis of podocytes (74). Podocyte insulin resistance can impact the morphological adjustment of podocytes in response to postprandial alterations of glomerular filtration rate (68). Podocytes apoptosis is prevalent in patients with obesity-related glomerulopathy and can cause further loss of podocytes and segmental glomerulosclerosis due to increased mechanical strain on remaining podocytes (75, 76).

Hypertrophy of proximal tubular epithelial cells has been observed in obesity, probably in response to increased hemodynamic and metabolic load (77). Moreover, increased absorption of luminal NEFA-bound albumin and basolateral plasma NEFA in obesity leads to the accumulation of NEFA in proximal epithelial tubular cells (68). The tubular NEFA overload enhances renal gluconeogenesis by interfering with tubular insulin signaling and eventually induces tubulointerstitial injury (78, 79).

Imaging-based quantification

Currently proton magnetic resonance spectroscopy (^{1}H-MRS) is the only noninvasive technique to quantify lipid content in vivo, and has been applied to measure the content of triglyceride in liver (80), muscle (81) and myocardium (82) with sufficient accuracy for clinical assessment (83). Unlike magnetic resonance imaging, which provides anatomical information based on signals of water, ^{1}H-MRS provides a biochemical assay of tissue in selected regions based on spatially encoded chemical information (84). The feasibility and reproducibility of renal triglyceride content measurement in human with ^{1}H-MRS has been shown at 1.5T (85) and 3.0T (86), respectively. In addition, the ^{1}H-MRS measured renal triglyceride content has been validated in a porcine study against gold-standard enzymatic assay (87).

Dixon fat/water images in three directions are usually obtained for better planning before the ^{1}H-MRS scan. A single voxel is placed in the renal parenchyma carefully avoiding perirenal fat and sinus fat (**Figure 2.14**). The kidney is an organ with low lipid content. Overall lipid content only comprises 0.6% to 1.64% of normal kidney weight (88). Pathological studies have estimated that in normal human kidney, 1/5 of the lipid content is triglyceride, 1/10 is NEFA, and cholesterol concentration is 1/20 or less (88, 89). Renal spectra obtained by ^{1}H-MRS mainly originates from the proton resonances of methylene (CH2) groups of triglyceride (**Figure 2.14**). Cholesterol also contains CH2 groups, but is less magnetic susceptible and results in resonance loss in clinical ^{1}H-MRS. Therefore, the lipid content quantified by ^{1}H-MRS is predominantly triglyceride content. In healthy young volunteers, total cortical triglyceride content is around 0.44% (85). The percentage of renal triglyceride varies with different scanners and scan protocols,

and studies of larger scale are needed to determine the normal references.

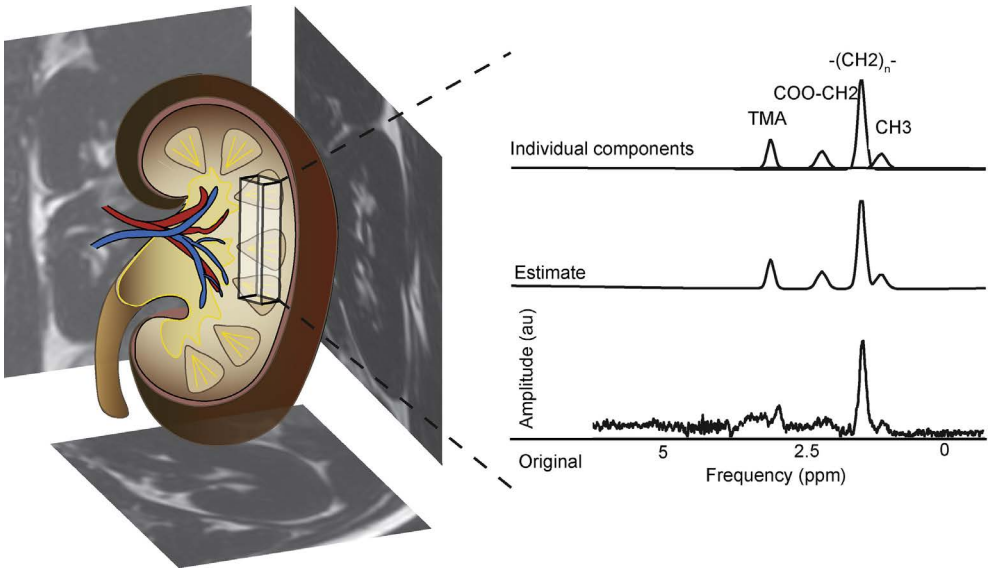

Figure 2.14 Single-voxel ^{1}H-MRS is planned in renal parenchyma avoiding perirenal and sinus fat (left). Corresponding spectra with methylene –$(CH2)_n$– peak between 1.2-1.4 ppm (right). TMA, trimethylamines. Reprinted from a published article (90) under a Creative Commons license.

CLINICAL IMPLICATIONS OF EXCESSIVE KIDNEY FAT

Fat around the kidney has been helpful in conventional diagnostic radiology for localizing renal lesions and staging of renal tumors. In the past decade, the research interests in kidney fat have been shifted to its association with chronic kidney disease, insulin resistance and cardiovascular diseases in the context of obesity. In addition, the clinical implications of perirenal fat has been studied in urological operations, nephrolithiasis and cancer.

Association with chronic kidney disease and insulin resistance

Obesity and diabetes mellitus developed in the context of obesity has become the leading cause of chronic kidney disease (91). The clinical and pathologic characteristics and pathogenesis of obesity-related glomerulopathy have been thoroughly illustrated in a previous review article (91). Accumulation of perirenal fat, renal sinus fat and renal triglyceride content has been found in obese patients with or without type 2 diabetes

mellitus (T2DM) (14, 22, 42, 90). Studies of the tissue samples collected from patients who underwent urological surgeries suggested that perirenal fat may contribute locally to the regulation of kidney function through chronic inflammation (54). In non-hypertensive and non-diabetic obese patients, larger perirenal fat thickness was found in patients with microalbuminuria than those with normoalbuminuria (36). Moreover, perirenal fat thickness was independently associated with urinary albumin/creatinine ratio, indicating its potential utility in predicting early kidney damage (36). Excessive perirenal fat was found to be associated with reduced glomerular filtration rate (GFR) in patients with T2DM (35, 43) as well as in patients with hypertension (39). Furthermore, perirenal fat thickness showed a higher predictive value for chronic kidney disease than subcutaneous and visceral fat in patients with T2DM (50).

Similar results have been reported in regard to renal sinus fat. In a non-diabetic cohort at diabetic risk, excessive renal sinus fat was found to be associated with exercise-induced albuminuria, independent of age, sex and VAT (57). In a mixed cohort of lean and obese participants, renal sinus fat volume was positively associated with the level of kidney injury factor (KIM)-1 and fibroblast growth factor (FGF)-21, which are serum biomarkers of kidney injury (19). Another study showed that in the presence of non-alcoholic fatty liver disease, the elevated hepatokine fetuin-A may impair renal function through increased renal sinus fat (58). In the Framingham Study, "fatty kidney" defined by renal sinus fat larger than 90% of a healthy reference sample, was associated with higher odds ratio of chronic kidney disease and diabetes mellitus, even after adjustment for VAT (92). A recent study reported that renal sinus fat volume was negatively associated with gold-standard GFR, but positively associated with renal vascular resistance in patients with T2DM (60). Our own study also found that sinus fat volume was positively associated with glycated hemoglobin and urinary albumin/creatinine ratio in patients with T2DM (14).

Association with cardiovascular diseases

Both perirenal fat and sinus fat have been associated with hypertension(40, 93) and calcified atherosclerosis (49, 55). It is proposed that excessive perirenal fat and sinus fat can induce mechanical compression of the renal parenchyma, vasculatures, nerve fibers and the collecting system, which subsequently stimulates the renin-angiotensin-aldosterone system and sympathetic nerves system. All these mechanisms lead to increased sodium reabsorption and contribute to hyperfiltration and hypertension (94). In addition, perirenal adipose tissue can secret all components of renin-angiotensin-aldosterone system, as well as a number of adipokines and cytokines directly linked to vasoactivity and endothelial function (6). As aforementioned, excessive perirenal fat

and sinus fat are also associated with microalbuminuria, which is a robust risk factor for cardiovascular diseases.

A positive association between para- and peri-renal fat thickness measured by ultrasonography and 24-hour diastolic blood pressure has been reported in a cohort of overweight and obese subjects, independent of anthropometric, hormonal and metabolic parameters (38). A study of 284 morbidly obese patients reported a larger thickness of perirenal fat in hypertensive patients than in non-hypertensive ones (40). In a cohort of 3929 participants, perirenal fat thickness derived from CT was associated with arterial calcification in renal artery and abdominal aorta after adjustment for multiple confounders (49). Moreover, studies in healthy (41) and overweight children (15) have reported a positive association between perirenal fat size and carotid intima-media thickness.

In the Framingham Study, renal sinus fat was associated with higher odds ratio of hypertension, even after adjustment for BMI or VAT (92). Renal sinus fat was significantly associated with the number of prescribed antihypertensive medications and stage II hypertension in participants at risk for cardiovascular events, even after accounting for several potential confounders including intraperitoneal fat (20). The ratio of renal sinus fat versus VAT was proposed as an independent risk indicator of coronary artery calcification in a study of middle-aged patients with suspected coronary artery disease (55).

Implications for other diseases

The quantification of perirenal fat can also be beneficial for pre-operational evaluations of nephrectomy, nephrolithiasis and cancer. The thickness of perirenal fat measured on CT images can be used to calculate the Mayo adhesive probability score (95), which has been helpful in predicting adherent perinephric fat in partial nephrectomy (51, 95-97). A study of laparoscopic donor nephrectomy found that CT-measured perirenal fat was positively associated with operative complexity as reflected by operative time (17). A recent study reported that the posterior thickness of perirenal fat measured on transversal CT was an independent predictor of postoperative complications after laparoscopic distal gastrectomy for patients with gastric cancer (98). Larger volume of perirenal fat was found around calcium oxalate stone-bearing kidneys than kidneys without stones in a cohort of 40 patients with nephrolithiasis (53). Due to the proximity of perirenal fat to the kidney and its paracrine function, there might be unique impact of prerenal fat on renal parenchymal tumors. It was demonstrated in 174 patients with clear cell renal carcinoma that perirenal fat size was correlated with local progression and life expectancy (99) (**Figure 2.15**). This potential utility of perirenal fat measurement

in decision-making for renal tumors might be extended to ovarian cancer, as a study in 258 patients demonstrate the association between perirenal adiposity and lower progression-free survival from ovarian cancer (100).

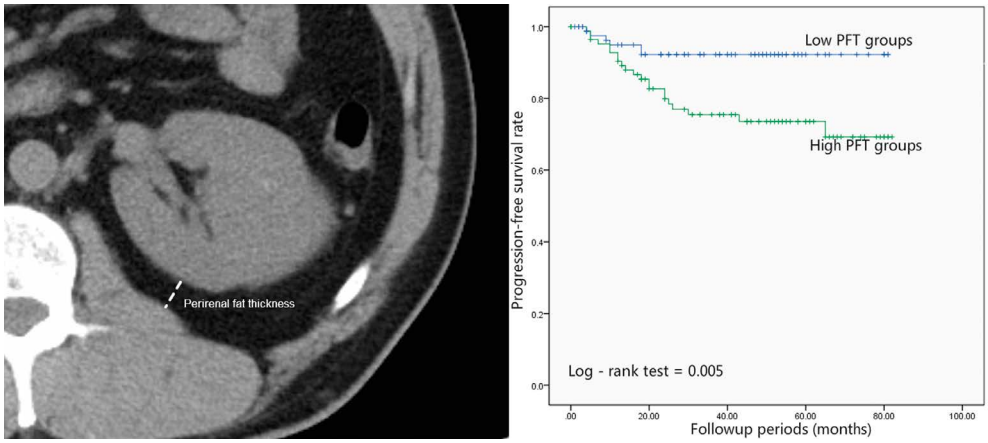

Figure 2.15 Perirenal fat thickness measured at the level of renal hilum using axial CT images (left) was associated with the progression-free survival in patients with localized clear cell renal cell carcinoma (right). High perirenal fat thickness (green line) predicted a poorer progression-free survival than low perirenal fat thickness (blue line). Reprinted from a published article (99) with permission from Elsevier.

Changes of excessive kidney fat after intervention

Most previous clinical studies of excessive kidney fat were cross-sectional in design. Longitudinal studies regarding the changes of excessive kidney fat after intervention are scarce and in relatively small sample size (19, 59, 90). In the aforementioned study of morbidly obese patients, 89 patients who underwent sleeve-gastrectomy showed a significant decrease of perirenal fat thickness as well as antihypertensive medications needed (40). Interestingly, controversial results have been reported regarding the change of renal sinus fat after anti-obesity intervention. One study found no significant reduction of renal sinus fat when VAT significantly (>5%) decreased (19), while another study demonstrated a decrease in renal sinus fat after an 18-month weight loss trial (59). As for intra-renal fat, a recent study demonstrated decreased renal triglyceride content quantified by ^{1}H-MRS after 26-week glycemic control in patients with T2DM (90).

SUMMARY AND PERSPECTIVES

Perirenal fat and renal sinus fat are smaller in size than the general abdomnal adipose compartments. Lipid accumulation in renal parenchyma is also lower than other organs capable of storing ectopic fat, such as liver. However, fat accumulation around and within the kidney directly participates in the regulation of kidney function, lipids metabolism, gluconeogenesis and cardiovascular homeostasis, which may have a unique role in the development of obesity-related diseases independent of the general visceral adipose tissue. There has been a lack of early-onset biomarkers for the clinical management of obesity-related chronic kidney disease and cardiovascular diseases. Excessive kidney fat may have a role in the pathogenesis of obesity-related diseases and is potentially reversable after intervention. Therefore, imaging-based quantification of perirenal fat, renal sinus fat and renal triglyceride content may bring new opportunities for early diagnosis and prognosis of obesity-related diseases. However, large-scale and longitudinal studies are required before these imaging biomarkers can be implemented in clinical practice. Furthermore, it remains unclear whether excessive fat around the kidney (perirenal and sinus fat) is associated with intra-renal lipid accumulation and to what degree they contribute to different disease entities.

Perirenal fat thickness measured by ultrasonography might be preferable for large-scale population studies, however the interobserver reproducibility remains to be validated. CT or MRI based quantification is more accurate and reproducible, especially for longitudinal studies. Considering the challenge of delineating renal fascia and the radiation risk from CT, volumetric quantification of renal sinus fat based on high-resolution MRI might be preferable for the evaluation of the fat accumulation around the kidneys in future studies. Finally, the utility of ^{1}H-MRS for the quantification of renal triglyceride content might gradually increase with the rising interests in intra-renal lipid, similar to that for the liver and the heart. With the development of artificial intelligence, imaging-based quantification of kidney fat might be simplified via deep-learning algorithms. Interdisciplinary collaboration among endocrinologists, nephrologists and radiologists is essential for further investigations of excessive kidney fat, and may contribute to improved clinical management of obesity-related diseases in the future.

REFERENCES

1. Gerota D. Beitrage zur kenntnis des befestigungsapparates der niere. Arch Anat Entwicklungsgesch. 1895;19:265-86.
2. Zuckerkandl E. Uber den Fixationsapaparat der Nieren. Med Jahrb. 1883:59-67.
3. Thornton FJ, Kandiah SS, Monkhouse WS, et al. Helical CT evaluation of the perirenal space and its boundaries: a cadaveric study. Radiology. 2001;218(3):659-63.
4. Marx WJ, Patel SK. Renal fascia: its radiographic importance. Urology. 1979;13(1):1-7.
5. Raptopoulos V, Touliopoulos P, Lei Q, et al. Medial border of the perirenal space: CT and anatomic correlation. Radiology. 1997;205(3):777-84.
6. Liu B-X, Sun W, Kong X-Q. Perirenal fat: a unique fat pad and potential target for cardiovascular disease. Angiology. 2019;70(7):584-93.
7. Meyers MA, Friedenberg RM, King MC, et al. The significance of the renal capsular arteries. The British journal of radiology. 1967;40(480):949-56.
8. Grigoraș A, Balan RA, Căruntu I-D, et al. Perirenal Adipose Tissue—Current Knowledge and Future Opportunities. Journal of Clinical Medicine. 2021;10(6):1291.
9. Czaja K, Kraeling R, Klimczuk M, et al. Distribution of ganglionic sympathetic neurons supplying the subcutaneous, perirenal and mesentery fat tissue depots in the pig. Acta neurobiologiae experimentalis. 2002;62(4):227-34.
10. Czaja K, Lakomy M, Kaleczyc J, et al. Leptin receptors, NPY, and tyrosine hydroxylase in autonomic neurons supplying fat depots in a pig. Biochemical and biophysical research communications. 2002;293(3):1138-44.
11. Kaissling B. Structural analysis of the rabbit kidney. 1979.
12. Montani J-P, Carroll JF, Dwyer TM, et al. Ectopic fat storage in heart, blood vessels and kidneys in the pathogenesis of cardiovascular diseases. International Journal of Obesity. 2004;28(4):S58-S65.
13. Caglar V, Songur A, Acar M, et al. Volumetric evaluation of fat in the renal sinus in normal subjects using stereological method on computed tomography images and its relationship with body composition. Folia Morphol. 2014;73(3):302-8.
14. Lin L, Dekkers IA, Huang L, et al. Renal sinus fat volume in type 2 diabetes mellitus is associated with glycated hemoglobin and metabolic risk factors. Journal of Diabetes and its Complications. 2021:107973.
15. Bassols J, Martinez-Calcerrada JM, Prats-Puig A, et al. Perirenal fat is related to carotid intima-media thickness in children. International Journal of Obesity. 2018;42(4):641-7.
16. Eisner BH, Zargooshi J, Berger AD, et al. Gender differences in subcutaneous and perirenal fat distribution. Surgical and Radiologic Anatomy. 2010;32(9):879-82.
17. Anderson KM, Lindler TU, Lamberton GR, et al. Laparoscopic donor nephrectomy: effect of perirenal fat upon donor operative time. Journal of endourology. 2008;22(10):2269-74.
18. Favre G, Grangeon-Chapon C, Raffaelli C, et al. Perirenal fat thickness measured with computed tomography is a reliable estimate of perirenal fat mass. Plos One. 2017;12(4):e0175561.

19. Krievina G, Tretjakovs P, Skuja I, et al. Ectopic Adipose Tissue Storage in the Left and the Right Renal Sinus is Asymmetric and Associated With Serum Kidney Injury Molecule-1 and Fibroblast Growth Factor-21 Levels Increase. Ebiomedicine. 2016;13:274-83.

20. Chughtai HL, Morgan TM, Rocco M, et al. Renal sinus fat and poor blood pressure control in middle-aged and elderly individuals at risk for cardiovascular events. Hypertension. 2010;56(5):901-6.

21. Dwyer TM, Banks SA, Alonso-Galicia M, et al. Distribution of renal medullary hyaluronan in lean and obese rabbits. Kidney international. 2000;58(2):721-9.

22. Notohamiprodjo M, Goepfert M, Will S, et al. Renal and renal sinus fat volumes as quantified by magnetic resonance imaging in subjects with prediabetes, diabetes, and normal glucose tolerance. Plos One. 2020;15(2):e0216635.

23. Chau Y-Y, Bandiera R, Serrels A, et al. Visceral and subcutaneous fat have different origins and evidence supports a mesothelial source. Nature cell biology. 2014;16(4):367-75.

24. Schleinitz D, Krause K, Wohland T, et al. Identification of distinct transcriptome signatures of human adipose tissue from fifteen depots. European Journal of Human Genetics. 2020;28(12):1714-25.

25. TANUMA Y, OHATA M, ITO T, et al. Possible function of human brown adipose tissue as suggested by observation on perirenal brown fats from necropsy cases of variable age groups. Archivum histologicum japonicum. 1976;39(2):117-45.

26. Jespersen NZ, Feizi A, Andersen ES, et al. Heterogeneity in the perirenal region of humans suggests presence of dormant brown adipose tissue that contains brown fat precursor cells. Molecular metabolism. 2019;24:30-43.

27. Svensson PA, Lindberg K, Hoffmann JM, et al. Characterization of brown adipose tissue in the human perirenal depot. Obesity (Silver Spring). 2014;22(8):1830-7.

28. Efremova A, Senzacqua M, Venema W, et al. A large proportion of mediastinal and perirenal visceral fat of Siberian adult people is formed by UCP1 immunoreactive multilocular and paucilocular adipocytes. Journal of physiology and biochemistry. 2020;76(2):185-92.

29. van den Beukel JC, Grefhorst A, Hoogduijn MJ, et al. Women have more potential to induce browning of perirenal adipose tissue than men. Obesity. 2015;23(8):1671-9.

30. Chen X, McClusky R, Chen J, et al. The number of x chromosomes causes sex differences in adiposity in mice. PLoS genetics. 2012;8(5):e1002709.

31. Foster MT, Pagliassotti MJ. Metabolic alterations following visceral fat removal and expansion: Beyond anatomic location. Adipocyte. 2012;1(4):192-9.

32. Hartman AD. Adipocyte fatty acid mobilization in vivo: effects of age and anatomical location. Lipids. 1985;20(5):255-61.

33. Hammoud SH, AlZaim I, Al-Dhaheri Y, et al. Perirenal Adipose Tissue Inflammation: Novel Insights Linking Metabolic Dysfunction to Renal Diseases. Frontiers in Endocrinology. 2021;12(942).

34. Mende CW, Einhorn D. Fatty kidney disease: a new renal and endocrine clinical entity? Describing the role of the kidney in obesity, metabolic syndrome, and type 2 diabetes. Endocrine Practice. 2019;25(8):854-8.

35. Lamacchia O, Nicastro V, Camarchio D, et al. Para- and perirenal fat thickness is an independent predictor of chronic kidney disease, increased renal resistance index and hyperuricaemia in type-2 diabetic patients. Nephrology Dialysis Transplantation. 2010;26(3):892-8.

36. Sun X, Han F, Miao W, et al. Sonographic evaluation of para-and perirenal fat thickness is an independent predictor of early kidney damage in obese patients. International urology and nephrology. 2013;45(6):1589-95.

37. Sahin SB, Durakoglugil T, Ayaz T, et al. Evaluation of para-and perirenal fat thickness and its association with metabolic disorders in polycystic ovary syndrome. Endocrine Practice. 2015;21(8):878-86.

38. De Pergola G, Campobasso N, Nardecchia A, et al. Para- and perirenal ultrasonographic fat thickness is associated with 24-hours mean diastolic blood pressure levels in overweight and obese subjects. BMC Cardiovasc Disord. 2015;15(1):108.

39. Geraci G, Zammuto MM, Mattina A, et al. Para-perirenal distribution of body fat is associated with reduced glomerular filtration rate regardless of other indices of adiposity in hypertensive patients. J Clin Hypertens. 2018;20(10):1438-46.

40. Ricci MA, Scavizzi M, Ministrini S, et al. Morbid obesity and hypertension: The role of perirenal fat. The Journal of Clinical Hypertension. 2018;20(10):1430-7.

41. López-Bermejo A, Prats-Puig A, Osiniri I, et al. Perirenal and epicardial fat and their association with carotid intima-media thickness in children. Annals of Pediatric Endocrinology & Metabolism. 2019;24(4):220.

42. Manno C, Campobasso N, Nardecchia A, et al. Relationship of para- and perirenal fat and epicardial fat with metabolic parameters in overweight and obese subjects. Eat Weight Disord. 2019;24(1):67-72.

43. Fang Y, Xu YC, Yang YX, et al. The Relationship between Perirenal Fat Thickness and Reduced Glomerular Filtration Rate in Patients with Type 2 Diabetes. Journal of Diabetes Research. 2020;2020.

44. Grima P, Guido M, Zizza A, et al. Sonographically measured perirenal fat thickness: An early predictor of atherosclerosis in HIV-1-infected patients receiving highly active antiretroviral therapy? Journal of Clinical Ultrasound. 2010;38(4):190-5.

45. Grima P, Guido M, Chiavaroli R, et al. Ultrasound-assessed perirenal fat is related to increased ophthalmic artery resistance index in HIV-1 patients. Cardiovascular ultrasound. 2010;8(1):1-9.

46. D'Marco L, Salazar J, Cortez M, et al. Perirenal fat thickness is associated with metabolic risk factors in patients with chronic kidney disease. Kidney research and clinical practice. 2019;38(3):365.

47. Roever L, Resende ES, Veloso FC, et al. Perirenal Fat and Association With Metabolic Risk Factors The Uberlandia Heart Study. Medicine. 2015;94(38):e1105.

48. Favre G, Grangeon-Chapon C, Raffaelli C, et al. Perirenal fat thickness measured with computed tomography is a reliable estimate of perirenal fat mass. Plos One. 2017;12(4):e0175561.

49. Koo BK, Denenberg JO, Wright CM, et al. Associations of Perirenal Fat Thickness with Renal and Systemic Calcified Atherosclerosis. Endocrinol Metab (Seoul). 2020;35(1):122-31.

50. Chen X, Mao Y, Hu J, et al. Perirenal fat thickness is significantly associated with the risk for development of chronic kidney disease in diabetic patients. Diabetes. 2021.

51. Ji C, Tang S, Yang K, et al. Analysis of Factors Influencing Mayo Adhesive Probability Score in Partial Nephrectomy. Med Sci Monit. 2017;23:6026-32.

52. Foster MC, Hwang SJ, Porter SA, et al. Development and reproducibility of a computed tomography-based measurement of renal sinus fat. BMC Nephrol. 2011;12(1):52.

53. Lama DJ, Safiullah S, Yang A, et al. Three-dimensional evaluation of perirenal fat volume in patients with nephrolithiasis. Urolithiasis. 2018;46(6):535-41.

54. Maimaituxun G, Fukuda D, Izaki H, et al. Levels of Adiponectin Expression in Peri-Renal and Subcutaneous Adipose Tissue and Its Determinants in Human Biopsied Samples. Front Endocrinol (Lausanne). 2019;10:897.

55. Murakami Y, Nagatani Y, Takahashi M, et al. Renal sinus fat volume on computed tomography in middle-aged patients at risk for cardiovascular disease and its association with coronary artery calcification. Atherosclerosis. 2016;246:374-81.

56. Lin P, Min Z, Wei G, et al. Volumetric evaluation of renal sinus adipose tissue on computed tomography images in bilateral nephrolithiasis patients. International urology and nephrology. 2020;52(6):1027-34.

57. Wagner R, Machann J, Lehmann R, et al. Exercise-induced albuminuria is associated with perivascular renal sinus fat in individuals at increased risk of type 2 diabetes. Diabetologia. 2012;55(7):2054-8.

58. Wagner R, Machann J, Guthoff M, et al. The protective effect of human renal sinus fat on glomerular cells is reversed by the hepatokine fetuin-A. Sci Rep. 2017;7(1):2261.

59. Zelicha H, Schwarzfuchs D, Shelef I, et al. Changes of renal sinus fat and renal parenchymal fat during an 18-month randomized weight loss trial. Clin Nutr. 2018;37(4):1145-53.

60. Spit KA, Muskiet MHA, Tonneijck L, et al. Renal sinus fat and renal hemodynamics: a cross-sectional analysis. MAGMA. 2020;33(1):73-80.

61. Rha SE, Byun JY, Jung SE, et al. The renal sinus: pathologic spectrum and multimodality imaging approach. Radiographics. 2004;24 Suppl 1:S117-31.

62. Nikolaidis P, Gabriel H, Khong K, et al. Computed tomography and magnetic resonance imaging features of lesions of the renal medulla and sinus. Curr Probl Diagn Radiol. 2008;37(6):262-78.

63. Ma J. Dixon techniques for water and fat imaging. J Magn Reson Imaging. 2008;28(3):543-58.

64. Rickards E. Remarks on the fatty transformation of the kidney. British medical journal. 1883;2(1175):2.

65. Björntorp P. " Portal" adipose tissue as a generator of risk factors for cardiovascular disease and diabetes. Arteriosclerosis: An Official Journal of the American Heart Association, Inc. 1990;10(4):493-6.

66. Steinberg D, Parthasarathy S, Carew TE, et al. Beyond cholesterol. New England Journal of Medicine. 1989;320(14):915-24.

67. Straub BK, Gyoengyoesi B, Koenig M, et al. Adipophilin/perilipin-2 as a lipid droplet-specific marker for metabolically active cells and diseases associated with metabolic

dysregulation. Histopathology. 2013;62(4):617-31.

68. De Vries AP, Ruggenenti P, Ruan XZ, et al. Fatty kidney: emerging role of ectopic lipid in obesity-related renal disease. The lancet Diabetes & endocrinology. 2014;2(5):417-26.

69. Ruan XZ, Varghese Z, Powis SH, et al. Human mesangial cells express inducible macrophage scavenger receptor. Kidney international. 1999;56(2):440-51.

70. Li J, Li H, Wen Y-b, et al. Very-low-density lipoprotein-induced triglyceride accumulation in human mesangial cells is mainly mediated by lipoprotein lipase. Nephron Physiology. 2008;110(1):p1-p10.

71. Chen Y, Ruan XZ, Li Q, et al. Inflammatory cytokines disrupt LDL-receptor feedback regulation and cause statin resistance: a comparative study in human hepatic cells and mesangial cells. American Journal of Physiology-Renal Physiology. 2007;293(3):F680-F7.

72. Ruan XZ, Varghese Z, Powis SH, et al. Dysregulation of LDL receptor under the influence of inflammatory cytokines: a new pathway for foam cell formation. Kidney international. 2001;60(5):1716-25.

73. Lennon R, Pons D, Sabin MA, et al. Saturated fatty acids induce insulin resistance in human podocytes: implications for diabetic nephropathy. Nephrology Dialysis Transplantation. 2009;24(11):3288-96.

74. Sieber J, Lindenmeyer MT, Kampe K, et al. Regulation of podocyte survival and endoplasmic reticulum stress by fatty acids. American journal of physiology-renal physiology. 2010;299(4):F821-F9.

75. Verani RR. Obesity-associated focal segmental glomerulosclerosis: pathological features of the lesion and relationship with cardiomegaly and hyperlipidemia. American journal of kidney diseases. 1992;20(6):629-34.

76. Fukuda A, Chowdhury MA, Venkatareddy MP, et al. Growth-dependent podocyte failure causes glomerulosclerosis. Journal of the American society of nephrology. 2012;23(8):1351-63.

77. Tobar A, Ori Y, Benchetrit S, et al. Proximal tubular hypertrophy and enlarged glomerular and proximal tubular urinary space in obese subjects with proteinuria. Plos One. 2013;8(9):e75547.

78. Tiwari S, Singh RS, Li L, et al. Deletion of the insulin receptor in the proximal tubule promotes hyperglycemia. Journal of the American Society of Nephrology. 2013;24(8):1209-14.

79. Yamahara K, Kume S, Koya D, et al. Obesity-mediated autophagy insufficiency exacerbates proteinuria-induced tubulointerstitial lesions. Journal of the American Society of Nephrology. 2013;24(11):1769-81.

80. Thomas EL, Hamilton G, Patel N, et al. Hepatic triglyceride content and its relation to body adiposity: a magnetic resonance imaging and proton magnetic resonance spectroscopy study. Gut. 2005;54(1):122-7.

81. Boesch C, Machann J, Vermathen P, et al. Role of proton MR for the study of muscle lipid metabolism. NMR in Biomedicine: An International Journal Devoted to the Development and Application of Magnetic Resonance In vivo. 2006;19(7):968-88.

82. van der Meer RW, Lamb HJ, Smit JW, et al. MR imaging evaluation of cardiovascular

risk in metabolic syndrome. Radiology. 2012;264(1):21-37.

83. Kamba M, Meshitsuka S, Iriguchi N, et al. Measurement of relative fat content by proton magnetic resonance spectroscopy using a clinical imager. Journal of Magnetic Resonance Imaging: An Official Journal of the International Society for Magnetic Resonance in Medicine. 2000;11(3):330-5.

84. Preul MC, Caramanos Z, Collins DL, et al. Accurate, noninvasive diagnosis of human brain tumors by using proton magnetic resonance spectroscopy. Nature medicine. 1996;2(3):323-5.

85. Hammer S, de Vries AP, de Heer P, et al. Metabolic imaging of human kidney triglyceride content: reproducibility of proton magnetic resonance spectroscopy. Plos One. 2013;8(4):e62209.

86. Dekkers IA, de Heer P, Bizino MB, et al. (1) H-MRS for the assessment of renal triglyceride content in humans at 3T: A primer and reproducibility study. J Magn Reson Imaging. 2018;48(2):507-13.

87. Jonker JT, de Heer P, Engelse MA, et al. Metabolic imaging of fatty kidney in diabesity: validation and dietary intervention. Nephrol Dial Transplant. 2018;33(2):224-30.

88. Druilhet RE, Overturf ML, Kirkendall WM. Cortical and medullary lipids of normal and nephrosclerotic human kidney. International Journal of Biochemistry. 1978;9(10):729-34.

89. Druilhet R, Overturf M, Kirkendall W. Structure of neutral glycerides and phosphoglycerides of human kidney. International Journal of Biochemistry. 1975;6(12):893-901.

90. Dekkers IA, Bizino MB, Paiman EHM, et al. The Effect of Glycemic Control on Renal Triglyceride Content Assessed by Proton Spectroscopy in Patients With Type 2 Diabetes Mellitus: A Single-Center Parallel-Group Trial. J Ren Nutr. 2020.

91. D'Agati VD, Chagnac A, de Vries AP, et al. Obesity-related glomerulopathy: clinical and pathologic characteristics and pathogenesis. Nat Rev Nephrol. 2016;12(8):453-71.

92. Foster MC, Hwang SJ, Porter SA, et al. Fatty kidney, hypertension, and chronic kidney disease: the Framingham Heart Study. Hypertension. 2011;58(5):784-90.

93. Mazairac AH, Joles JA. Renal sinus adiposity and hypertension. Am Heart Assoc; 2010.

94. Hall ME, do Carmo JM, da Silva AA, et al. Obesity, hypertension, and chronic kidney disease. International journal of nephrology and renovascular disease. 2014;7:75.

95. Davidiuk AJ, Parker AS, Thomas CS, et al. Mayo adhesive probability score: an accurate image-based scoring system to predict adherent perinephric fat in partial nephrectomy. European urology. 2014;66(6):1165-71.

96. Martin L, Rouviere O, Bezza R, et al. Mayo adhesive probability score is an independent computed tomography scan predictor of adherent perinephric fat in open partial nephrectomy. Urology. 2017;103:124-8.

97. Dariane C, Le Guilchet T, Hurel S, et al., editors. Prospective assessment and histological analysis of adherent perinephric fat in partial nephrectomies. Urologic Oncology: Seminars and Original Investigations; 2017: Elsevier.

98. Eto K, Ida S, Ohashi T, et al. Perirenal fat thickness as a predictor of postoperative

complications after laparoscopic distal gastrectomy for gastric cancer. BJS open. 2020;4(5):865-72.

99. Huang H, Chen S, Li W, et al., editors. High perirenal fat thickness predicts a poor progression-free survival in patients with localized clear cell renal cell carcinoma. Urologic Oncology: Seminars and Original Investigations; 2018: Elsevier.

100. Zhang Y, Coletta AM, Allen PK, et al. Perirenal adiposity is associated with lower progression-free survival from ovarian cancer. International Journal of Gynecologic Cancer. 2018;28(2).

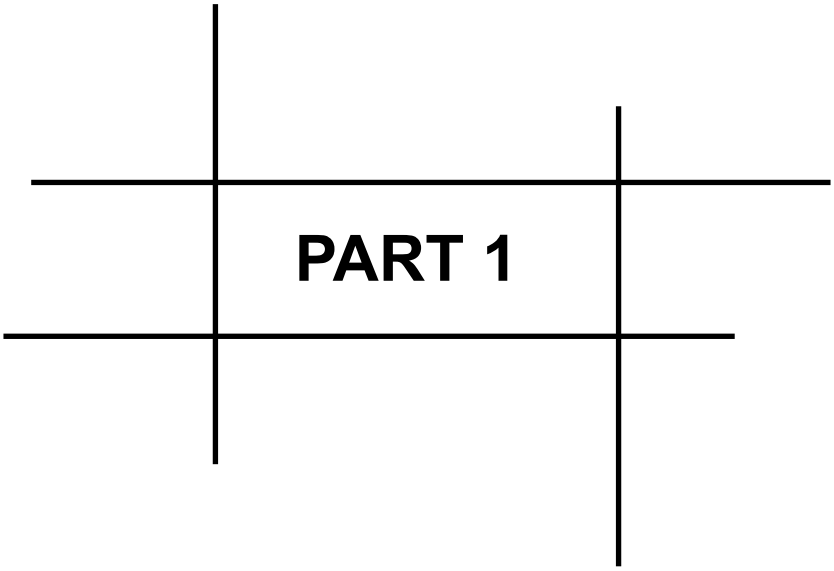

Clinical Studies on Visceral/Renal Fat